

Acute and Chronic Effects of Noninvasive Ventilation on Left and Right Myocardial Function in Patients with Obstructive Sleep Apnea Syndrome: A Speckle Tracking Echocardiographic Study

Antonello D'Andrea, M.D., Ph.D.,* Francesca Martone, M.D.,* Biagio Liccardo, MD., Ph.D.,* Mariano Mazza, M.D.,† Anna Annunziata, M.D.,† Enza Di Palma, M.D.,* Marianna Conte, M.D.,* Cesare Sirignano, M.D.,¶ Michele D'Alto, M.D.,* Nicolino Esposito, M.D.,‡ Giuseppe Fiorentino, M.D.,† Maria Giovanna Russo, M.D.,* Eduardo Bossone, M.D., Ph.D.,§ and Raffaele Calabrò, M.D.*

*Chair of Cardiology, Second University of Naples, Monaldi Hospital-AORN Ospedali dei Colli, Naples, Italy; †Division of Pneumology, Second University of Naples, Monaldi Hospital-AORN Ospedali dei Colli, Naples, Italy; ‡Division of Cardiology, Evangelic Hospital Villa Betania, Naples, Italy; §Department of Cardiology and Cardiac Surgery, University Hospital San Giovanni di Dio e Ruggi d'Aragona, Salerno, Italy; and ¶Institute of Biostructure and Bioimaging (IBB) of the Italian National Research Council, Naples, Italy

Background: In patients with obstructive sleep apnea syndrome (OSAS), repetitive hypoxia due to sleep-induced apnea adversely affects the interaction between myocardial oxygen demand and supply, resulting in the development of subclinical cardiac dysfunction. The purpose of the study was to analyze the different involvement of left and right heart myocardial function in patients with OSAS treated with noninvasive ventilation (NIV). **Methods:** Conventional Doppler echocardiography, Doppler myocardial imaging (DMI), and two-dimensional speckle tracking echocardiography (2DSTE) of left (LV) and right ventricular (RV) longitudinal and right atrial (RA) deformation were performed in 55 patients with OSAS undergoing NIV (M/F 38/17; mean age 67.8 ± 11.2 years). LV and RV global longitudinal strain (GLS) was calculated by averaging local strain along the entire right and left ventricle, before and during NIV, and after 6 months of nocturnal NIV therapy. **Results:** LV morphology was comparable before and during NIV, whereas LV ejection fraction and LV DMI early diastolic peak velocity were significantly improved in patients with OSAS during NIV, as was LV regional peak myocardial strain ($P < 0.001$). RV diameters were slightly increased in patients with OSAS during ventilation, whereas pulmonary artery systolic pressure (PASP), RV GLS, and regional peak myocardial RV strain were significantly reduced during ventilation ($P < 0.0001$). RA transverse diameters and RA area were also slightly increased during NIV, whereas RA lateral wall strain was reduced ($P < 0.001$). Acute RV myocardial impairment completely reversed at follow-up, with a decrease in PASP and subsequent increase in both RV and RA myocardial performance. **Conclusions:** Conventional 2DSTE is a useful tool for assessing left and right heart morphology and myocardial deformation in patients with OSAS and for monitoring both acute and chronic effects of NIV. (Echocardiography 2016;33:1144–1155)

Key words: obstructive sleep apnea syndrome, Doppler echocardiography, noninvasive ventilation, pulmonary arterial pressure, right ventricle, two-dimensional speckle tracking strain

Obstructive sleep apnea syndrome (OSAS) is characterized by repeated episodes of partial or complete obstruction of the upper airways during sleep, resulting in apnea and hypopnea periods, oxygen desaturation, frequent nocturnal arousals, and daytime sleepiness.^{1,2} It has

become an increasing health problem associated with a variety of cardiovascular disorders,^{3,4} including left (LV) and right ventricular (RV) dysfunction, hypertension, coronary artery disease, heart failure, hypertrophy, and arrhythmias.^{2,5} In particular, in patients with OSAS, repetitive hypoxia due to sleep-induced obstructive apnea adversely affects the interaction between myocardial oxygen demand and supply, with subsequent development of subclinical LV systolic dysfunction.⁶

Continuous positive airway pressure (CPAP) is a proven therapy for OSAS and it is known to

Address for correspondence and reprint requests: Antonello D'Andrea, M.D., Ph.D., Via M. Schipa 44, 80122 Naples, Italy. Fax: +39 0817064234;

E-mail: antonellodandrea@libero.it

[Correction added on August 15, 2016, after first online publication: The fifth author's name was changed from Anna Nunziata to Anna Annunziata.]

maintain upper airway patency during sleep by increasing transmural pressure.⁷ CPAP was also found to improve cardiac function in patients with OSAS.⁸

Among various echocardiographic techniques, a novel approach to quantify regional myocardial deformation from routine grayscale two-dimensional (2D) echocardiographic images, known as 2D speckle tracking echocardiography (2DSTE), calculates myocardial strain independent of angle of incidence and has been used to assess LV and RV deformation in different clinical settings.^{9,10}

On these grounds, the aim of this study was to assess by means of 2DSTE the involvement of RV and LV myocardial function in patients with OSAS treated with noninvasive ventilation (NIV).

Methods:

Study Population:

From January 2014 to July 2014, 67 patients with OSAS were first referred to the Divisions of Cardiology and Pneumology of the Second University of Study of Naples, Monaldi Hospital (Naples, Italy), for clinical and instrumental screening, and then to our echocardiographic laboratory for this study. All patients underwent detailed history, physical examination, electrocardiogram, arterial blood gas (ABG) analysis before and during NIV, overnight polysomnography (PSG), and comprehensive transthoracic echocardiography, including Doppler and strain studies. Exclusion criteria were coronary artery disease, valvular or congenital heart disease, bicuspid aortic valve, congestive heart failure, cardiomyopathies, and inadequate echocardiographic image quality. According to these criteria, 12 subjects were excluded (3 for Duchenne muscular dystrophy with severe dilated cardiomyopathy, 3 for amyotrophic lateral sclerosis, 4 for death and impossibility to perform imaging during ventilation, and 2 for poor echocardiographic image quality).

Forty-five age- and sex-matched subjects without detectable cardiovascular disease were also enrolled. Volunteer controls were all recruited in Naples (Italy) and selected from our departments of Cardiology among subjects investigated for work eligibility and were examined in a single center (Monaldi Hospital, Naples, Italy). None of the control subjects had cardiovascular structural or functional abnormalities or received any medication.

Therefore, our final study population consisted of 100 subjects. The study was approved by the local ethics committee, and all subjects gave informed consent.

Sleep Study:

Overnight PSG was performed in the sleep laboratory using standard recording techniques

(Compumedics Sleep Diagnostic system E-series PSG Compumedics, Abbotsford, Australia) and ProFusion PSG. Airflow was monitored using an air pressure sensor placed at the nose with thermistor placed at the nose and mouth, whereas arterial oxygen saturation (SaO₂) was recorded continuously using a pulse oximeter. Arousals were scored according to accepted definitions. Sleep stages were scored according to the standard criteria of the American Academy of Sleep Medicine. Apneas were defined as complete cessation of inspiratory airflow for at least 10 second. Hypopnea was defined as a significant reduction (>50%) in respiratory signals for at least 10 second associated with an arousal or reduction in SaO₂ of more than 3% of baseline value. The apnea-hypopnea index (AHI) was defined as the number of apnea and/or hypopnea events per hour of sleep. Patients with an AHI of five times per hour or more were considered to have OSAS.¹

Imaging Protocol:

Standardized transthoracic echocardiography and Doppler examinations were performed with commercially available equipment in all subjects (Vivid E9, GE Healthcare, Milwaukee, WI, USA) before and during the first CPAP trial, and after 6 months of nocturnal CPAP therapy. All studies were reviewed and analyzed off line by two independent observers blinded to the clinical characteristics of the study population. The average of 3–5 cardiac cycles was used for specific measurements.

M- and B-Mode Measurements:

M-mode measurements, including LV diastolic and systolic diameters, interventricular septum, and posterior wall thickness, were performed in parasternal long-axis view with the patient in the left lateral position. Relative diastolic wall thickness was determined as the ratio between twice the posterior wall thickness and LV end-diastolic diameter.¹¹ RV end-diastolic chamber size was accurately assessed according to the recent American Society of Echocardiography guidelines for the echocardiographic assessment of the right heart in adults.¹² In particular, three parameters included measurement of basal, mid-cavity, and longitudinal diameters from the apical four-chamber view at end-diastole. RV wall thickness was measured in diastole, preferably from the subcostal view, using either M-mode or 2D imaging.¹²

Tricuspid annular plane systolic excursion (TAPSE) was used as an index of RV longitudinal systolic function by placing an M-mode cursor through the tricuspid annulus and measuring the amount of longitudinal motion of the annulus at peak systole (in mm) in the standard apical four-

chamber view.¹³ Right atrial (RA) measurements were assessed in the apical four-chamber view. Maximum RA diameter was defined from the mid-level of the RA free wall to the interatrial septum. RA area was estimated by planimetry at the end of ventricular systole (largest volume), tracing from the lateral aspect of the tricuspid annulus to the septal aspect, excluding the area between the leaflets and annulus, following the RA endocardium.¹²

Color Doppler Analysis:

Valvular regurgitation was quantified from color Doppler imaging.¹⁴ Doppler-derived LV diastolic inflow was recorded in the apical four-chamber view by placing the sample volume at the tips of the tricuspid valve. LV diastolic measurements included E and A peak velocities (in m/s).¹¹ The early (Em) and late (Am) diastolic velocities were measured at the septal and lateral corner of the mitral annulus by pulsed-Doppler myocardial imaging (DMI). In order to obtain a measure of RV myocardial function using DMI, RV peak systolic velocity (Sm) was assessed from the apical four-chamber view by placing the sample volume at the tricuspid annulus. Because this technique uses Doppler, special care is required to ensure optimal image orientation and avoid underestimation of velocities.¹²

Noninvasive Pulmonary Artery Systolic Pressure:

Tricuspid regurgitation peak velocity was measured from the spectral profile of the tricuspid regurgitant jet in the RV inflow projection of the parasternal long- or short-axis view, or apical four-chamber view. The highest transvalvular velocity was used for calculation of RV systolic pressure. According to the American Society of Echocardiography recommendations,¹² right atrial pressure (RAP) was estimated by the inferior vena cava (IVC) respiratory index. Pulmonary artery systolic pressure (PASP) was then calculated by adding the value of RAP to the systolic transtricuspid gradient according to the following formula:

$$\text{PASP} = 4V^2 + \text{RAP}$$

where V is maximal velocity of the tricuspid regurgitant jet and PASP was assumed to equate RV systolic pressure in the absence of pulmonic stenosis and/or RV outflow tract obstruction.^{15,16}

Non-Doppler Two-Dimensional Strain Imaging:

Two-dimensional strain uses grayscale (B-mode) sector images and is based on frame-by-frame tracking of small rectangular image blocks with stable speckle pattern. A minimum frame rate of 30 Hz was required for reliable operation of this

program, and frame rates of 60–90 Hz were used for routine grayscale imaging. Apical four-chamber view (the same as RV diameter measurement) was obtained using the same ultrasound system and the probe used for conventional echocardiography; end-systole was chosen as the single frame for the endocardial-to-epicardial region of interest to include maximal wall thickness for strain calculation. A region of interest was traced on the endocardial cavity interface of the apical four-chamber view at left atrial and RV systole (minimum cavity area) by a point-and-click approach. Then, a second larger region was automatically generated near the epicardium with a width of 10 mm. The tracking process and conversion to Lagrangian strains were performed offline using dedicated software (Echo-PAQ PC 2D strain, GE Healthcare, Milwaukee, WI, USA). Longitudinal strains for each individual segment were measured and averaged. In addition, the software calculated LV and RV global longitudinal strain (GLS) by averaging local strains along the entire ventricles^{17–19} (Figs 1 and 2).

Non-Doppler RA strain analysis was also performed for the basal segment of the RA lateral walls in the four-chamber apical view. Continuous care was taken to keep the sample volume out of the vena cava. A circular region of interest was traced onto the RA endocardial cavity interface of the apical four-chamber view at RV systole, by a point-and-click approach. Then, a second larger concentric circle was automatically generated near the epicardium with a default width of 15 mm. The region of interest included the entire RA myocardial walls, and a click feature increased or decreased the width of the circles for thicker or thinner walls, respectively.

Arterial Blood Gas Analysis:

All patients underwent arterial samples before and during NIV, and ABG analysis thereafter. Measurement of pH, pCO₂, bicarbonate, and oxygen saturation by co-oximetry (SaO₂ or SvO₂) was taken for each sample, using an Instrumentation Laboratory Blood Gas Analyzer IL1620. PH, pCO₂, and pO₂ were measured directly, whereas actual plasma bicarbonate (HCO₃⁻), lactate, SaO₂, and other additional parameters were derived mathematically.

Noninvasive Ventilation:

All patients underwent NIV through an oro-facial mask or helmet with the application of positive end-expiratory pressure (PEEP) for at least 12 hours.

Statistical Methods:

All statistical analyses were performed with SPSS 18.0 for Windows (SPSS Inc., Chicago, IL, USA). Variables are presented as mean±SD. Two-tailed

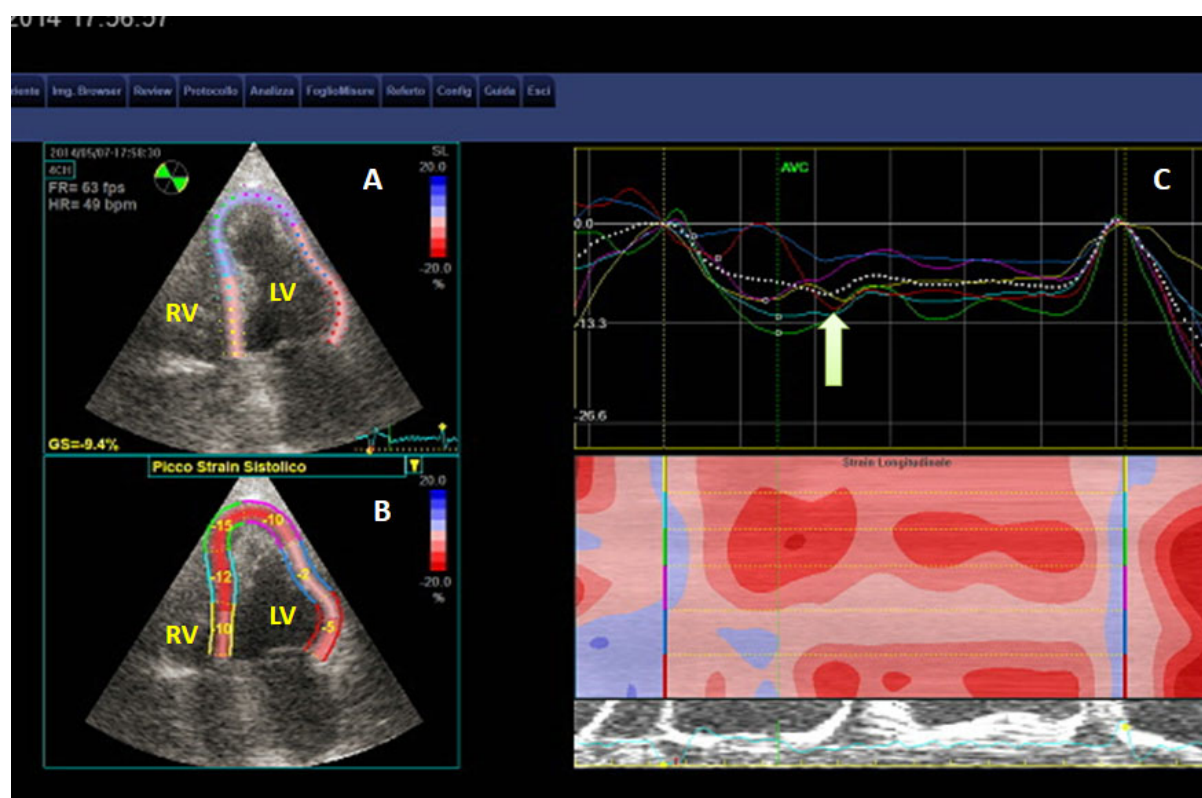


Figure 1. Left ventricular speckle tracking strain analysis in a patient with obstructive sleep apnea syndrome showing impairment of left ventricular global longitudinal strain **A**, and regional myocardial function **B**, as documented by strain curves **C**.

t-test for unpaired data and ANOVA test for repeated measures were used to assess changes between groups (patients with OSAS vs. controls; patients with OSAS before and during ventilation and at follow-up). Linear regression analysis and partial correlation test by Pearson's method were carried out to assess univariate relations. To identify significant independent determinants of the main LV, RV, and RA myocardial strain indexes, individual association with clinically relevant and echocardiographic variables was assessed by multivariate Cox linear regression analysis. The following variables were included in the analysis: clinical data (age, gender, weight, height, body mass index [BMI]), standard echocardiographic LV and RV indexes, ABG parameters, and PSG. These variables were selected according to clinical relevance and potential impact on RV function. Variable selection was performed in the multivariate linear regression as an interactive stepwise backward elimination method, each time excluding the one variable with the highest *P*-value according to Wald statistics. In order to minimize type 1 error rate inflation due to multiple testing, statistical significance was defined as a two-sided *P*-value <0.01.

Receiver operating characteristic (ROC) curve analysis was performed to select optimal cutoff

values of echocardiographic measurements. Reproducibility of 2DSTE measurements was determined in all subjects. Intra-observer variability was assessed using both Pearson's bivariate two-tailed correlations and Bland-Altman analysis. Correlation coefficients, 95% confidence intervals (CIs), and percent errors were reported.

Results:

Overall, 100 patients were included in the study. Similarly to previous reports,^{1,3,4} patients with OSAS were mainly older males with significantly increased BMI and a large prevalence of arterial hypertension. Cardiovascular risk factors and medical therapy of the whole study population are reported in Table I.

Standard Echocardiography and Two-Dimensional Strain Analysis at Baseline and during Noninvasive Ventilation:

Left heart: LV mass index was mildly increased in patients with OSAS. In particular, septal and posterior wall thicknesses were higher in patients with OSAS than in controls, as was LA volume index. In addition, patients with OSAS also showed a significant impairment of LV diastolic function and LV global and regional myocardial function (Tables II and III).

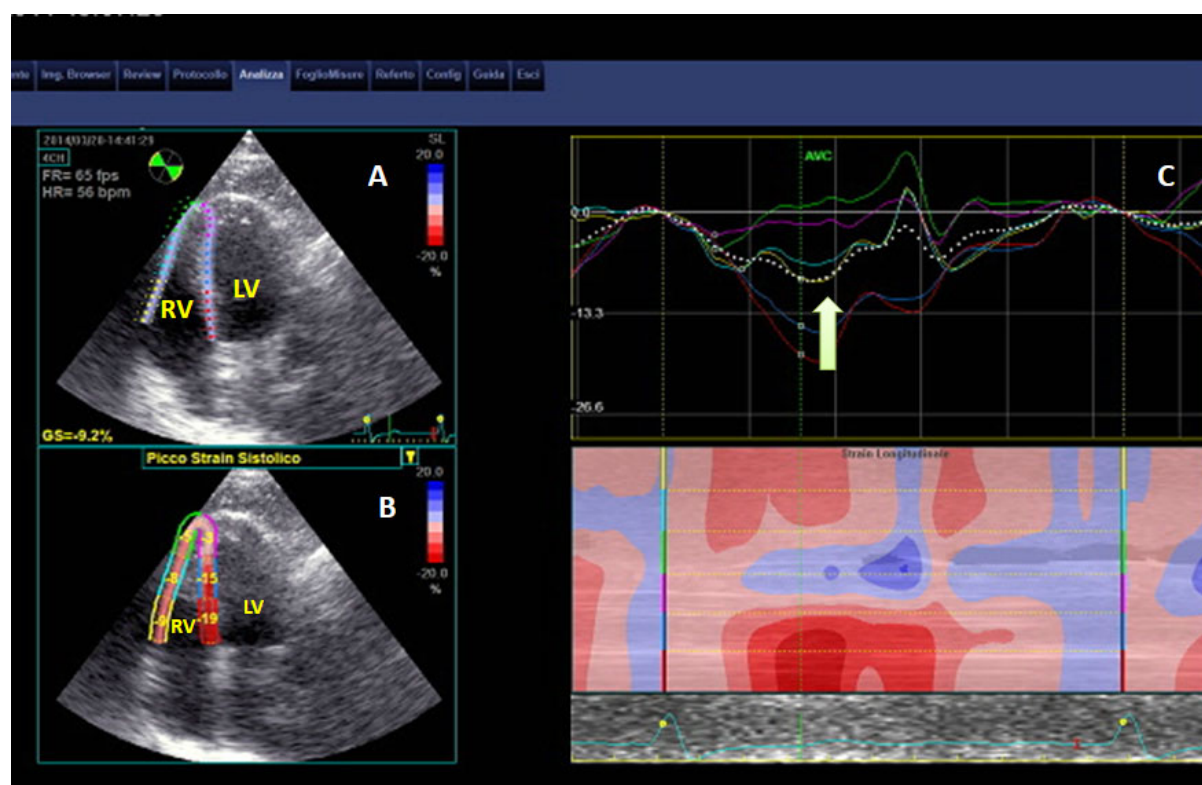


Figure 2. Right ventricular speckle tracking strain analysis in a patient with obstructive sleep apnea syndrome showing subclinical right ventricular myocardial impairment at a **A.** global and **B.** regional level, as documented by **C.** strain curves.

Overall, LV strain analysis was possible in 95% of 880 attempted segments from the patients with OSAS and in 97% of 720 attempted segments from the control subjects.

LV geometry was comparable before and during CPAP, whereas LV ejection fraction was slightly increased during ventilation. LV DMI E peak velocity of both basal septum and lateral wall was significantly improved during NIV, as was LV GLS and regional peak myocardial LV strain (Tables IV and V; Fig. 1).

Right heart: Overall, RV strain analysis was possible in 91% of 165 attempted segments from the patients with OSAS and in 95% of 135 attempted segments from the control subjects.

RV diameters and functional parameters at baseline were comparable between patients with OSAS and controls, whereas an increase in pulmonary pressure was observed in the former. No differences were found in RV morphology, TAPSE, and RV Sm before and during ventilation. Conversely, IVC diameter in both inspiration and expiration and PASP were higher during NIV (Table IV), and RV GLS and regional peak myocardial RV strain (basal, mid-, and apical segments) were significantly impaired in patients

with OSAS during CPAP, as was RA lateral wall strain (Table V; Fig. 2).

Arterial Blood Gases:

Arterial blood gases changed during ventilation and at follow-up, with a significant improvement in pH, pO_2 , and SaO_2 and reduced pCO_2 (Table VI). NIV also reduced blood lactate and bicarbonate concentrations.

Follow-Up Study after Chronic CPAP Treatment:

No weight loss occurred in patients with OSAS from baseline to follow-up (BMI: 33.6 ± 6.6 vs. 33.3 ± 2.5 kg/m², $p=NS$) as well as no changes in medication. All patients were interviewed after 6 months of CPAP therapy, and 6-8 months thereafter. The level of CPAP pressure required to eliminate apnea was computed from a second overnight PSG performed within 5 weeks of the first sleep study. The first CPAP application was well tolerated by all patients and was used on a nightly basis. All patients were initially placed on CPAP with only 3 patients unable to tolerate it at follow-up.

A significant improvement in AHI (from 35.1 ± 15.4 to 5.1 ± 8.2 /h, $P < 0.001$), mini-

TABLE I
Demographic and Clinical Characteristics of the Study Population

Variable	OSAS (n = 55)	Controls (n = 45)
Age (years)	67.8 ± 11.2	65.9 ± 12.3
Sex (M/F)	38/17 (69.9%)	32/13 (71.1%)
Weight (kg)	92.8 ± 20.6*	84.6 ± 19.3
Height (cm)	167.8 ± 8.5	168.3 ± 6.5
Heart rate (bpm)	75.6 ± 10.8	73.9 ± 11.7
Body mass index (kg/m ²)	33.6 ± 6.6*	28.7 ± 3.6
Systolic blood pressure (mmHg)	138.8 ± 8.3 [†]	130.2 ± 4.3
Diastolic blood pressure (mmHg)	88.4 ± 7.3 [†]	81.6 ± 4.3
Family history of CAD (n)	22	—
Systemic hypertension (n)	30	—
Diabetes mellitus (n)	19	—
Hypercholesterolemia (n)	16	—
Obesity (n)	42	—
Smoker (n)	18	—
Previous smoker (n)	10	—
Chronic artery disease (n)	8	—
Medical therapy (n)		
ACEi	22	—
ARB	7	—
β-blockers	11	—
Corticosteroids	11	—
β-adrenergic agonists	15	—
Oxygen therapy (n)	5	—
Apnea–hypopnea index (/h)	35.1 ± 15.4	—
Total sleep time (min)	375.5 ± 78.3	—
Minimal SaO ₂ (%)	82.6 ± 7.8	—
<90% saturation time (min)	23.5 ± 33.9	—

ACEi = angiotensin converting enzyme inhibitor; ARB = angiotensin receptor antagonist; CAD = coronary artery disease; OSAS = obstructive sleep apnea syndrome; SaO₂ = arterial oxygen saturation.

*P < 0.001.

[†]P < 0.01.

mal SaO₂ (from 82.6 ± 7.8% to 91.1 ± 6.2%, P < 0.001), and ABG parameters was observed after chronic CPAP therapy (Table VI).

Of note, the acute reduction in RV longitudinal strain during NIV was no longer detectable at follow-up. Repeated echocardiographic analysis revealed a significant decrease in PASP and a parallel improvement in RV strain indexes with chronic CPAP use. Conversely, no significant increase was recorded in LV myocardial indexes between acute and chronic CPAP.

On univariate analysis, RV GLS during ventilation was found to significantly correlate with blood lactate concentration before ventilation (r = 0.75, P < 0.0001), AHI (r = 0.62, P < 0.0001), history of cigarette smoking, and PASP before ventilation (r = 0.65, P < 0.0001). On the other hand, LV GLS during ventilation was found to significantly correlate with blood lactate concentration before ventilation (r = 0.48, P < 0.001) and history of diabetes mellitus.

On multivariate analysis, after adjusting for potential determinants, the independent associa-

tion of RV GLS with blood lactate concentration before NIV (β-coefficient: 0.59; P < 0.001), AHI (β-coefficient: 0.48; P < 0.001), and PASP (β: 0.53; P < 0.001) and the independent correlation between LV GLS and blood lactate concentration before ventilation (β-coefficient: 0.35, P < 0.01) were confirmed.

By ROC curve analysis, a 2D strain RV GLS cut off point of −14% better differentiated patients with severe OSAS (AHI >20/h) from controls (sensitivity 83.5%, specificity 92.3%).

Reproducibility of Left and Right Ventricular Global Longitudinal Strain Measurements:

Intra-observer variability: Pearson's correlation: LV GLS: r = 0.91, P < 0.00001; RV GLS: r = 0.87, P < 0.00001.

Bland–Altman analysis: LV GLS (95% CI ±1.2; percent error 3.1%), RV GLS (95% CI ±1.4; percent error 3.5%).

Inter-observer variability: Pearson's correlation: LV GLS: r = 0.88, P < 0.00001; RV GLS: r = 0.84, P < 0.00001.

TABLE II
Baseline Left and Right Heart Standard Echo Doppler Variables

Variable	OSAS (n = 55)	Controls (n = 45)	P
Septal wall thickness (mm)	11.2 ± 1.3	8.9 ± 2.1	<0.01
LV posterior wall thickness (mm)	10.4 ± 1.2	8.4 ± 1.1	<0.01
LV end-diastolic diameter (mm)	49.4 ± 4.7	48.2 ± 3.8	NS
LV end-systolic diameter (mm)	32.4 ± 3.8	33.6 ± 4.6	NS
LV ejection fraction (%)	56.2 ± 5.5	58.4 ± 6.5	NS
LV stroke volume (mL/b)	66.4 ± 4.3	68.9 ± 4.3	NS
LV mass index (g/m ^{2.7})	52.5 ± 3.3	48.4 ± 4.8	<0.001
Left atrial volume index (mL/m ²)	32.5 ± 4.6	28.5 ± 5.8	<0.001
RV diameter (4-ch annulus) (mm)	33.8 ± 4.5	31.3 ± 3.5	NS
RV diameter (4-ch middle ventricle) (mm)	30.8 ± 5.6	29.6 ± 4.7	NS
RV long-axis diameter (4-ch) (mm)	59.8 ± 8.3	61.8 ± 2.1	NS
RV wall thickness (mm)	4.3 ± 1.1	4.1 ± 4.2	NS
TAPSE (mm)	22.6 ± 2.2	23.8 ± 2.5	NS
IVC diameter inspiration (mm)	13.3 ± 4.8	12.6 ± 3.5	NS
IVC diameter expiration (mm)	19.3 ± 4.6	18.8 ± 3.9	NS
RA transverse diameter (mm)	39.8 ± 5.4	37.8 ± 4.5	NS
RA area (cm ²)	19.3 ± 4.6	17.9 ± 5.5	NS
Transmitral E-wave (m/s)	0.61 ± 0.24	0.67 ± 0.33	<0.05
Transmitral A-wave (m/s)	0.72 ± 0.32	0.68 ± 0.55	NS
Transmitral E/A ratio	0.87 ± 0.3	0.97 ± 0.4	<0.01
Deceleration time (ms)	175.4 ± 14.5	155.6 ± 15.5	<0.01
E/Ea ratio	8.2 ± 0.4	6.3 ± 3.7	<0.01
DMI LV Ea peak velocity basal septum (m/s)	0.09 ± 0.03	0.10 ± 0.05	NS
DMI LV A peak velocity basal septum (m/s)	0.14 ± 0.04	0.10 ± 0.06	NS
DMI LV Ea peak velocity basal lateral wall (m/s)	0.08 ± 0.05	0.10 ± 0.04	NS
DMI LV A peak velocity basal lateral wall (m/s)	0.14 ± 0.04	0.11 ± 0.07	NS
DMI RV Sm peak velocity (m/s)	0.11 ± 0.04	0.15 ± 0.06	NS
Tricuspid peak E velocity (m/s)	0.14 ± 0.04	0.12 ± 0.05	NS
Tricuspid peak A velocity (m/s)	0.13 ± 0.06	0.13 ± 0.07	NS
Tricuspid regurgitation velocity (m/s)	2.69 ± 0.76	2.18 ± 0.56	<0.001
PASP (mmHg)	35.8 ± 14.4	24.8 ± 11.3	<0.001

4-ch = four-chamber; DMI = Doppler myocardial imaging; IVC = inferior vena cava; IVRT = isovolumic relaxation time; LA = left atrial; LV = left ventricular; RA = right atrial; RV = right ventricular; TAPSE = tricuspid annular plane systolic excursion; OSAS = obstructive sleep apnea syndrome; PASP = pulmonary artery systolic pressure.

Bland–Altman analysis: LV GLS (95% CI ± 1.6; percent error 3.7%), RV GLS (95% CI ± 1.8; percent error 3.9%).

Discussion:

To the best of our knowledge, this is the first study that assessed LV, RV, and RA regional deformation using 2DSTE in patients with OSAS before and during NIV, as well as after chronic CPAP treatment. Our main findings show that (1) patients with OSAS have both subclinical LV and RV myocardial dysfunction as compared to age- and sex-matched healthy controls; (2) LV myocardial function is acutely improved during NIV, with persistent beneficial effects at follow-up; (3) RV and RA myocardial deformation acutely decreases during NIV, but such transient reduction is completely reversible, with progressive improvement after chronic CPAP treatment.

Left and Right Subclinical Myocardial Dysfunction in OSAS:

A close correlation between OSAS and LV systolic dysfunction has been reported in previous studies using pulsed DMI, demonstrating that OSAS is associated with sleep-induced LV systolic longitudinal dysfunction.²⁰ This is not surprising if we consider that patients with OSAS experience repeated increases in LV afterload during sleeping due to exaggerated negative intrathoracic pressure and intermittent hypoxia and arousal. Acute repeated increases in afterload can therefore result in LV subclinical systolic dysfunction.

However, DMI measurements depend heavily on the insonation angle of the ultrasound beam and thus cannot be obtained for all regions of both LV and RV walls. Conversely, in the present study, we used 2DSTE, an approach to quantify myocardial deformation within a scan plane that is inherently 2D and independent of

TABLE III

Baseline Left and Right Heart Strain Variables

Variable	OSAS (n = 55)	Controls (n = 45)	P
LV basal lateral wall mean 2DSTE (%)	-7.8 ± 4.4	-15.9 ± 5.4	<0.0001
LV mid-lateral wall mean 2DSTE (%)	-7.4 ± 7.6	-16.6 ± 7.3	<0.0001
LV apical lateral wall mean 2DSTE (%)	-10.6 ± 10.4	-15.7 ± 8.5	<0.001
LV basal septal wall mean 2DSTE (%)	-10.5 ± 4.4	-15.5 ± 6.4	<0.001
LV mid-septal wall mean 2DSTE (%)	-12.2 ± 4.8	-16.2 ± 5.8	<0.001
LV apical septal wall mean 2DSTE (%)	-14.1 ± 9.3	-17.1 ± 6.3	<0.001
LV GLS (%)	-11.5 ± 4.1	-16.8 ± 5.1	<0.001
RV basal lateral wall mean 2DSTE (%)	-15.7 ± 9.5	-18.8 ± 7.5	<0.01
RV mid-lateral wall mean 2DSTE (%)	-15.6 ± 8.7	-17.4 ± 5.7	<0.01
RV apical lateral wall mean 2DSTE (%)	-10.7 ± 10.5	-15.5 ± 6.5	<0.001
RV GLS (%)	-13.8 ± 5.2	-17.6 ± 5.6	<0.01
RA lateral wall 2DSTE (%)	38.5 ± 4.6	48.8 ± 10.6	<0.001

2DSTE = two-dimensional speckle tracking echocardiography; GLS = global longitudinal strain; LA = left atrial; LV = left ventricular; OSAS = obstructive sleep apnea syndrome; RA = right atrial; RV = right ventricular.

TABLE IV

Left and Right Heart Echocardiographic Variables at Baseline, during NIV, and after Chronic CPAP Therapy in Patients with OSAS

Variable	Baseline	During NIV	After Chronic CPAP
Septal wall thickness (mm)	11.2 ± 1.3	11.6 ± 1.1	10.9 ± 1.4
LV posterior wall thickness (mm)	10.4 ± 1.2	10.6 ± 1.1	10.2 ± 1.3
LV end-diastolic diameter (mm)	49.4 ± 4.7	48.6 ± 5.1	50.4 ± 3.7
LV ejection fraction (%)	56.2 ± 5.5*	59.7 ± 4.1	60.2 ± 5.1
RV diameter (4-ch annulus) (mm)	33.8 ± 4.5	34.9 ± 3.1	32.4 ± 5.5
RV diameter (4-ch middle ventricle) (mm)	30.8 ± 5.6	31.9 ± 5.9	29.9 ± 6.6
RV long-axis diameter (4-ch) (mm)	59.8 ± 8.3	59.4 ± 5.8	59.6 ± 5.3
TAPSE (mm)	22.6 ± 2.2	19.9 ± 3.6	22.8 ± 2.6
IVC diameter inspiration (mm)	13.3 ± 4.8	14.9 ± 5.6 [†]	12.9 ± 5.8
IVC diameter expiration (mm)	19.3 ± 4.6	22.9 ± 7.2 [†]	18.3 ± 4.6
RA transverse diameter (mm)	39.8 ± 5.4	41.60 ± 6.2	38.6 ± 3.2
RA area (cm ²)	19.3 ± 4.6	21.13 ± 4.2 [†]	18.3 ± 4.6
Transmitral E-wave (m/s)	0.61 ± 0.24	0.74 ± 0.3 [†]	0.67 ± 0.54 [§]
Transmitral A-wave (m/s)	0.72 ± 0.32	0.87 ± 0.3 [†]	0.68 ± 0.32
Transmitral E/A ratio	0.87 ± 0.3	0.85 ± 0.4	0.88 ± 0.5
LV E/Ea ratio	8.2 ± 0.4 [‡]	5.5 ± 0.5	5.1 ± 0.3
DMI LV Ea peak velocity basal septum (m/s)	0.09 ± 0.03 [‡]	0.14 ± 0.02	0.16 ± 0.04
DMI LV A peak velocity basal septum (m/s)	0.14 ± 0.04	0.13 ± 0.04	0.12 ± 0.08
DMI LV E peak velocity basal lateral wall (m/s)	0.08 ± 0.05 [‡]	0.15 ± 0.03	0.16 ± 0.05
DMI LV A peak velocity basal lateral wall (m/s)	0.14 ± 0.04	0.09 ± 0.04	0.09 ± 0.04
DMI RV Sm peak velocity (m/s)	0.12 ± 0.04	0.11 ± 0.06	0.13 ± 0.04
Tricuspid peak E velocity (m/s)	0.14 ± 0.04*	0.17 ± 0.03	0.16 ± 0.04
Tricuspid peak A velocity (m/s)	0.13 ± 0.06	0.16 ± 0.06	0.15 ± 0.06
Tricuspid regurgitation velocity (m/s)	2.69 ± 0.8	2.93 ± 0.7 [†]	2.53 ± 0.6 [§]
PASP(mmHg)	35.8 ± 14.4	42.8 ± 12.2 [†]	30.8 ± 12.2 [§]

CPAP = continuous positive airway pressure; DMI = Doppler myocardial imaging; IVC = inferior vena cava; IVRT = isovolumic relaxation time; LA = left atrial; LV = left ventricular; NIV = noninvasive ventilation; OSAS = obstructive sleep apnea syndrome; PASP = pulmonary artery systolic pressure; RA = right atrial; RV = right ventricular; TAPSE = tricuspid annular plane systolic excursion.

*P < 0.01 baseline versus acute NIV and chronic CPAP.

[†]P < 0.01 acute NIV versus baseline and chronic CPAP.

[‡]P < 0.001 baseline versus acute NIV and chronic CPAP.

[§]P < 0.05 chronic CPAP versus baseline.

TABLE V

Strain Echocardiographic Variables at Baseline, during NIV, and after Chronic CPAP Therapy in Patients with OSAS

Variable	Baseline	During NIV	After Chronic CPAP
LV basal lateral wall mean 2DSTE (%)	-7.8 ± 4.4*	-12.8 ± 6.9	-13.3 ± 4.6
LV mid-lateral wall mean 2DSTE (%)	-7.4 ± 7.6*	-9.9 ± 5.9	-10.2 ± 7.4
LV apical lateral wall mean 2DSTE (%)	-10.6 ± 10.4 [‡]	-14.6 ± 7.5	-14.8 ± 9.4
LV basal septal wall mean 2DSTE (%)	-10.5 ± 4.4 [‡]	-14.4 ± 4.9	-14.6 ± 5.4
LV mid-septal wall mean 2DSTE (%)	-12.2 ± 4.8*	-14.3 ± 6.1	-14.2 ± 5.5
LV apical septal wall mean 2DSTE (%)	-14.1 ± 9.3*	-16.6 ± 10.1	-14.1 ± 9.3
LV GLS (%)	-11.5 ± 4.1 [‡]	-14.3 ± 4.2	-14.8 ± 4.5
RV basal lateral wall mean 2DSTE (%)	-15.7 ± 9.5	-13.4 ± 8.3 [†]	-16.3 ± 7.8 [§]
RV mid-lateral wall mean 2DSTE (%)	-15.6 ± 8.7	-13.4 ± 7.5 [†]	-15.9 ± 9.2
RV apical lateral wall mean 2DSTE (%)	-10.7 ± 10.5	-7.3 ± 8.8 [†]	-11.2 ± 9.5 [§]
RV GLS (%)	-13.8 ± 5.2	-10.9 ± 4.9 [†]	-14.6 ± 6.2 [§]
RA lateral wall 2DSTE (%)	38.5 ± 4.6	35.4 ± 3.8 [†]	40.6 ± 4.8

CPAP = continuous positive airway pressure; 2DSTE = two-dimensional speckle tracking echocardiography; GLS = global longitudinal strain; LA = left atrial; LV = left ventricular; NIV = noninvasive ventilation; OSAS = obstructive sleep apnea syndrome; RA = right atrial; RV = right ventricular.

*P < 0.01 baseline versus acute NIV and chronic CPAP.

[†]P < 0.01 acute NIV versus baseline and chronic CPAP.

[‡]P < 0.001 baseline versus acute NIV and chronic CPAP.

[§]P < 0.05 chronic CPAP versus baseline.

TABLE VI

Arterial Blood Gases Before and during Ventilation and after Chronic CPAP in Patients with OSAS

Variable	Before NIV	During NIV	After Chronic CPAP
pH	7.32 ± 0.14*	7.38 ± 0.09	7.41 ± 0.05
pCO ₂ (mmHg)	55.3 ± 9.8*	51.2 ± 9.8	47.2 ± 9.8
pO ₂ (mmHg)	52.3 ± 11.1 [†]	66.1 ± 12.3	69.1 ± 11.3
SaO ₂ (%)	86.6 ± 6.6*	93.5 ± 3.5	94.6 ± 3.5
Blood lactate (mmol/L)	2.3 ± 1.7 [†]	1.4 ± 0.5	1.1 ± 0.5
Blood bicarbonate (mmol/L)	29.4 ± 6.1 [‡]	27.6 ± 4.7	25.5 ± 3.7

CPAP = continuous positive airway pressure; NIV = noninvasive ventilation; OSAS = obstructive sleep apnea syndrome; SaO₂ = arterial oxygen consumption.

*P < 0.001 baseline versus acute NIV and chronic CPAP.

[†]P < 0.0001 baseline versus acute NIV and chronic CPAP.

[‡]P < 0.05 baseline versus acute NIV and chronic CPAP.

interrogation angle as it tracks speckle patterns (acoustic markers) within serial B-mode sector scans.^{17, 18, 21–23}

Although several recent reports described LV DMI and 2D strain patterns in patients with OSAS, little is known about RV and RA 2D strain at baseline and during NIV. Our results confirm that patients with OSAS show both LV involvement and early RV myocardial dysfunction, which are closely associated with OSAS severity and blood lactate concentration before ventilation. The reasons for RV impairment in OSAS remain to be fully elucidated. In these patients, primary pulmonary disease resulting from intermittent nocturnal hypoxemia and hypercapnia, LV dysfunction, increased sympathetic activity, and systemic hypertension may all promote a

progressive impairment of RV diastolic and systolic function.^{7,8}

In patients with different stages of OSAS, Hammerstingl et al. found a significant correlation between regional and global RV strain parameters and OSAS severity, along with a remarkable increase in RV deformation capability after CPAP therapy. These data suggest that apical RV dysfunction might be a sensitive parameter to detect early and even subclinical changes in RV function.²⁴

Acute and Chronic Effects of Continuous Positive Airway Pressure on Left and Right Ventricular Function:

In agreement with previous reports showing better LV myocardial indexes during CPAP in

patients with OSAS,⁶ LV myocardial GLS and regional 2D strain peaks were significantly increased in our population in both the acute and chronic evaluation, suggesting a NIV-induced improvement in LV myocardial deformation. This is not surprising if we consider that, following CPAP therapy, obstruction in the upper respiratory tract reduces, snoring disappears, apnea and arousal diminish, oxygen saturation normalizes, excessive platelet activation decreases, sympathetic activity reduces, myocardial oxygen transport improves, and LV transmural pressure, afterload, and pulmonary arterial pressure fall.

Conversely, although traditional systolic indexes (e.g. TAPSE, DMI Sm) were in the normal range, our study demonstrates acute mild worsening of right heart deformation during NIV with PEEP, with complete reversal of transient RV dysfunction during follow-up.

Decreased RV GLS may partially result from abnormal RV diastolic filling, due to increased RV afterload and reduced venous return during NIV.

In healthy subjects, resting measures of RV mass and contractility are about one-third to one-fifth those of the left ventricle, and this appropriately matches the pressure requirements of each. This lesser RV myocardial mass suggests that it may have a diminished contractile reserve and may be less able to accommodate marked changes in loading. Recent studies showed that an increase in pulmonary artery pressure during prolonged intense exercise results in an increase in RV wall stress estimates of 125% as compared with a modest 14% increase in LV wall stress, with subsequent transient RV dysfunction.^{25,26}

As described in both animal and human experimental models, the primary effect of PEEP on the normal heart is a simultaneous increase in RV afterload and a decrease in preload.²⁷ In invasive studies, although LV systolic pressure falls with increasing levels of PEEP, RV systolic pressure increases. In addition, during NIV steady state, RV septal to free wall diameter remains relatively constant, whereas LV dimensions decrease significantly.^{27,28} If external compressive effects are the only factor involved, RV systolic pressure would fall as stroke volume declines. The finding of increasing RV systolic pressure in the presence of decreasing stroke volume implies a considerable increase in pulmonary vascular resistance as a consequence of airway pressure, with a reduction in the cross-sectional area of pulmonary arterioles and capillaries, consistent with the hypothesis of Whittenberger et al.²⁹ Therefore, the primary effect of airway pressure on the pulmonary circulation is to slightly increase mean pulmonary vascular resistance. However, in patients with OSAS, reduced RV chamber perfor-

mance may cause an acute improvement in LV myocardial deformation due to reduced pulmonary overload, with subsequent LV preload decrease and enhanced LV performance.

Similarly, our study also shows acute worsening of RA deformation during NIV, most likely resulting from increased RV afterload and, hence, impaired RV diastolic filling. As previously demonstrated by our group, lower measurement values of strain suggest a deteriorated left and right atrial function and progression of atrial remodeling.^{10,30}

Another key finding of our study is that chronic treatment with CPAP results in significantly decreased PASP and improved RV and RA function. This effect could not be attributed to a reduction in body weight, as BMI was unchanged. Several mechanisms may account for this finding, including reversal of hypoxia, abolition of apneas, and subsequent mechanical overload due to increased respiratory effort, suppression of reflex mechanisms that could affect the pulmonary vasculature, and improved LV function.

Our findings are consistent with those of Nahmias et al.,³¹ where RV dysfunction was detected in patients with OSAS using radionuclide ventriculography and improved after chronic CPAP therapy in obese patients. In addition, Cloward et al.³² showed regression of LV hypertrophy after 6 months of CPAP therapy, but no changes in left and right atrial enlargement were observed. Recent randomized controlled trials also revealed a reduction of up to 10 mmHg in systolic and diastolic pressure with CPAP therapy.^{33,34} In OSAS patients undergoing three-dimensional echocardiography, Oliveira et al. showed a reduction in pulmonary vascular resistance and an increase in RV ejection fraction (63.0 ± 7.2 to $70.8 \pm 0.9\%$) after 24 weeks of NIV treatment.³⁵ Finally, using cardiac magnetic resonance, Magalang et al. reported that CPAP therapy decreased RV volumes in patients with severe OSAS.³⁶

Study Limitations:

Our study has several limitations. This is the first report assessing RV function in patients with OSAS using 2DSTE. In particular, the EchoPAC PC program from GE HealthCare was used for 2D strain analysis. As a definite 2DSTE software for RV 2D strain has not yet been developed, a 2DSTE program for LV strain was applied to analyze also RV and RA strain.^{10,30,37} The feasibility and reproducibility of RV strain patterns and measurements were good.

The lack of a gold standard for assessing baseline RV function is another limitation. Although previous studies used TAPSE and DMI to assess

RV function, more data are needed, particularly in an attempt to correlate echocardiographic findings with invasive measures of RV function.²⁰

As there are no standard orthogonal RA views to use the apical biplane method for RA volume calculations and the single-plane area-length and method of disks formulas have only been applied to RA volume determination in a few small studies,³⁸ in accordance with previous reports,^{39,40} the RA area index was taken as a measurement of RA size, which proved highly feasible with good reproducibility.

The diastolic impairment we observed in baseline conditions in our patients with OSAS could be in part related to the effects of the obesity alone, as previously reported.^{41,42} What is more, it should be highlighted the observed substantial improvement in LV regional diastolic function after chronic CPAP therapy need to be confirmed in future studies involving a larger cohort of patients with OSAS.

Our study also lacks hemodynamic data. An assessment by right heart catheterization might have provided more accurate information about RV function and RAP.

A technical limitation is that STE is dependent on both frame rate and image resolution. The frame rate in our setting ranged from 50 to 90 frames/s; this value is lower than the frame rate available with Doppler strain. However, the RA deformation indexes used in our study did not rely on differences in the timing of contraction.

As for the analysis of global RV deformation, 2DSTE software cannot accurately separate LV septal from RV septal components; therefore, half of the global indexes may be determined by septal function. However, we assessed RV free wall longitudinal myocardial deformation, and RV global and regional involvement in patients with OSAS was comparable.

Finally, the sample size limited our ability to draw definitive conclusions regarding RV myocardial deformation in selected patients undergoing NIV.

Conclusions:

In this study, a novel speckle tracking algorithm applied to routine grayscale 2D images proved to be a promising and feasible noninvasive technique to assess LV and RV myocardial function in patients with OSAS before and after NIV treatment. Obese patients with OSAS who have either awake alveolar hypoventilation or severe sleep apnea are at risk of developing both LV and RV subclinical myocardial dysfunction. However, nightly use of CPAP not only decreases OSAS severity, but also improves sleep-induced longitudinal LV and RV function as assessed by 2DSTE,

and its use should therefore be strongly encouraged.

Ethical Approval:

All procedures performed in studies involving human participants were in accordance with the ethical standards of the institutional and/or national research committee and with the 1964 Helsinki Declaration and its later amendments or comparable ethical standards. Informed consent was obtained from all individual participants included in the study.

Acknowledgments:

The authors are grateful to Dr. Paola Luciolli for excellent scientific English review of the manuscript.

References

1. Association American Sleep Disorders: *International Classification of Sleep Disorders: Diagnostic and Coding Manual, revised*. Rochester, MN: American Sleep Disorders Association, 1997, pp. 177–180.
2. Bayram NA, Ciftci B, Bayram H, et al: Effects of continuous positive airway pressure therapy on right ventricular function assessment by tissue Doppler imaging in patients with obstructive sleep apnea syndrome. *Echocardiography* 2008;25:1071–1078.
3. Young T, Peppard PE, Gottlieb DJ: Epidemiology of obstructive sleep apnea: A population health perspective. *Am J Respir Crit Care Med* 2002;154:1217–1239.
4. Leung RS, Bradley TD: Sleep apnea and cardiovascular disease. *Am J Respir Crit Care Med* 2001;164:2147–2165.
5. Phillips B: Sleep-disordered breathing and cardiovascular disease. *Sleep Med Rev* 2005;9:131–140.
6. Haruki N, Takeuchi M, Kanazawa Y, et al: Continuous positive airway pressure ameliorates sleep-induced subclinical left ventricular systolic dysfunction: Demonstration by two-dimensional speckle-tracking echocardiography. *Eur J Echocardiogr* 2010;11:352–358.
7. Dursunoglu N, Dursunoglu D, Ozkurt S, et al: Effects of CPAP on right ventricular myocardial performance index in obstructive sleep apnea patients without hypertension. *Respir Res* 2006;7:22.
8. Mansfield DR, Gollogly NC, Kaye DM, et al: Controlled trial of continuous positive airway pressure in obstructive sleep apnea and heart failure. *Am J Respir Crit Care Med* 2004;169:361–366.
9. D'Andrea A, Stanzola A, Di Palma E, et al: Right ventricular structure and function in idiopathic pulmonary fibrosis with or without pulmonary hypertension. *Echocardiography* 2016;33:57–65.
10. D'Andrea A, Caso P, Romano S, et al: Different effects of cardiac resynchronization therapy on left atrial function in patients with either idiopathic or ischaemic dilated cardiomyopathy: A two-dimensional speckle strain study. *Eur Heart J* 2007;28:2738–2748.
11. Lang RM, Badano LP, Mor-Avi V, et al: Recommendations for cardiac chamber quantification by echocardiography in adults: An update from the American Society of Echocardiography and the European Association of Cardiovascular Imaging. *J Am Soc Echocardiogr* 2015;28:1–39.
12. Rudski LG, Lai WW, Afilalo J, et al: Guidelines for the echocardiographic assessment of the right heart in adults: A report from the American Society of Echocardiography endorsed by the European Association of

- Echocardiography, a registered branch of the European Society of Cardiology, and the Canadian Society of Echocardiography. *J Am Soc Echocardiogr* 2010;23:685–713.
13. Steiner S, Schannwell CM, Strauer BE: Left ventricular response to continuous positive airway pressure: Role of left ventricular geometry. *Respiration* 2008;76:393–397.
 14. Bonow RO, Carabello BA, Chatterjee K, et al: 2008 Focused update incorporated into the ACC/AHA 2006 guidelines for the management of patients with valvular heart disease: A report of the American College of Cardiology/American Heart Association Task Force on Practice Guidelines (Writing Committee to Revise the 1998 Guidelines for the Management of Patients With Valvular Heart Disease): Endorsed by the Society of Cardiovascular Anesthesiologists, Society for Cardiovascular Angiography and Interventions, and Society of Thoracic Surgeons. *Circulation* 2008;118:e523–e661.
 15. Abbas AE, Fortuin FD, Schiller NB, et al: A simple method for noninvasive estimation of pulmonary vascular resistance. *J Am Coll Cardiol* 2003;41:1021–1027.
 16. Bossone E, D'Andrea A, D'Alto M, et al: Echocardiography in pulmonary arterial hypertension: From diagnosis to prognosis. *J Am Soc Echocardiogr* 2013;26:1–14.
 17. Korinek J, Kjaergaard J, Sengupta PP, et al: High spatial resolution speckle tracking improves accuracy of 2-dimensional strain measurements: An update on a new method in functional echocardiography. *J Am Soc Echocardiogr* 2007;20:165–170.
 18. Dalen H, Thorstensen A, Aase SA, et al: Segmental and global longitudinal strain and strain rate based on echocardiography of 1266 healthy individuals: The HUNT study in Norway. *Eur J Echocardiogr* 2010;11:176–183.
 19. D'Andrea A, Caso P, Bossone E, et al: Right ventricular myocardial involvement in either physiological or pathological left ventricular hypertrophy: An ultrasound speckle-tracking two-dimensional strain analysis. *Eur J Echocardiogr* 2010;11:492–500.
 20. Gondi S, Dokainish H: Right ventricular tissue Doppler and strain imaging: Ready for clinical use? *Echocardiography* 2007;24:522–532.
 21. Severino S, Caso P, Cicala S, et al: Involvement of right ventricle in left ventricular hypertrophic cardiomyopathy: Analysis by pulsed tissue imaging. *Eur J Echocardiogr* 2000;1:281–288.
 22. D'Andrea A, Caso P, Severino S, et al: Different involvement of right ventricular myocardial function in either physiologic or pathologic left ventricular hypertrophy: A Doppler tissue study. *J Am Soc Echocardiogr* 2003;16:154–161.
 23. Yang HS, Mookadam F, Warsame TA, et al: Evaluation of right ventricular global and regional function during stress echocardiography using novel velocity vector imaging. *Eur J Echocardiogr* 2010;11:157–164.
 24. Hammerstingl C, Schueler R, Wiesen M, et al: Impact of untreated obstructive sleep apnea on left and right ventricular myocardial function and effects of CPAP therapy. *PLoS ONE* 2013;8:e76352.
 25. D'Andrea A, La Gerche A, Golia E, et al: Right heart structural and functional remodeling in athletes. *Echocardiography* 2015;32(Suppl 1):S11–S22.
 26. La Gerche A, Roberts T, Claessen G: The response of the pulmonary circulation and right ventricle to exercise: Exercise-induced right ventricular dysfunction and structural remodeling in endurance athletes. *Pulm Circ* 2014;4:407–416.
 27. Smith PK, Tyson GS Jr, Hammon JW Jr, et al: Cardiovascular effects of ventilation with positive expiratory airway pressure. *Ann Surg* 1982;195:121–130.
 28. Rankin JS, Olsen CO, Arentzen CE, et al: The effects of airway pressure on cardiac function in intact dogs and man. *Circulation* 1982;66:108–120.
 29. Whittenberger JL, McGregor M, Berglund E, et al: Influence of state of inflation of the lung on pulmonary vascular resistance. *J Appl Physiol* 1960;15:878–882.
 30. D'Andrea A, Caso P, Romano S, et al: Association between left atrial myocardial function and exercise capacity in patients with either idiopathic or ischemic dilated cardiomyopathy: A two-dimensional speckle strain study. *Int J Cardiol* 2009a;132:354–363.
 31. Nahmias J, Lao R, Karetzky M: Right ventricular dysfunction in obstructive sleep apnoea: Reversal with nasal continuous positive airway pressure. *Eur Respir J* 1996;9:945–951.
 32. Cloward TV, Walker JM, Farney RJ, et al: Left ventricular hypertrophy is a common echocardiographic abnormality in severe obstructive sleep apnea and reverses with nasal continuous positive airway pressure. *Chest* 2003;124:594–601.
 33. Faccenda JF, Mackay TW, Boon NA, et al: Randomized placebo controlled trial of continuous positive airway pressure on blood pressure in the sleep apnea-hypopnea syndrome. *Am J Respir Crit Care Med* 2002;163:344–348.
 34. Becker HF, Jerrentrup A, Ploch T, et al: Effect of nasal continuous positive airway pressure treatment on blood pressure in patients with obstructive sleep apnea. *Circulation* 2003;107:68–73.
 35. Oliveira W, Poyares D, Cintra F, et al: Impact of continuous positive airway pressure treatment on right ventricle performance in patients with obstructive sleep apnoea, assessed by three-dimensional echocardiography. *Sleep Med* 2012;13:510–516.
 36. Magalang UJ, Richards K, McCarthy B, et al: Continuous positive airway pressure therapy reduces right ventricular volume in patients with obstructive sleep apnea: A cardiovascular magnetic resonance study. *J Clin Sleep Med* 2009;5:110–114.
 37. Di Salvo G, Drago M, Pacileo G, et al: Atrial function after surgical and percutaneous closure of atrial septal defect: A strain rate imaging study. *J Am Soc Echocardiogr* 2005;18:930–933.
 38. Raymond RJ, Hinderliter AL, Willis PW, et al: Echocardiographic predictors of adverse outcomes in primary pulmonary hypertension. *J Am Coll Cardiol* 2002;39:1214–1219.
 39. D'Andrea A, Salerno G, Scarafile R, et al: Right ventricular myocardial function in patients with either idiopathic or ischemic dilated cardiomyopathy without clinical sign of right heart failure: Effects of cardiac resynchronization therapy. *Pacing Clin Electrophysiol* 2009b;32:1017–1029.
 40. D'Andrea A, Scarafile R, Riegler L, et al: Right atrial size and deformation in patients with dilated cardiomyopathy undergoing cardiac resynchronization therapy. *Eur J Heart Fail* 2009c;11:1169–1177.
 41. Mureddu GF, De Simone G, Greco RG, et al: Left ventricular filling pattern in uncomplicated obesity. *Am J Cardiol* 1996;77:5.
 42. Russo C, Jin Z, Homma S, et al: Effect of obesity and overweight on left ventricular diastolic function. *J Am Coll Cardiol* 2011;57:1368–1374.